

## Comprehensive study of electronic polarizability and band gap of $B_2O_3$ - $Bi_2O_3$ - $ZnO$ - $SiO_2$ glass network

Iskandar Shahrin Mustafa<sup>\*,†,¶</sup>, Nur Ain Nabilah Razali<sup>\*,||</sup>,  
Nurul Zahirah Noor Azman<sup>\*,†,\*\*</sup>, Nor Zakiah Yahaya<sup>‡,††</sup>,  
Muhammad Zulhafiz Mohamad Zaini<sup>\*,‡‡</sup>, Nur Lina Rusli<sup>\*,§§</sup>,  
Muhammad Bakhsh Nizamani<sup>\*,¶</sup> and Halimah Mohamed Kamari<sup>§,||||</sup>

<sup>\*</sup>*School of Physics, University of Science Malaysia  
11800 USM, Pulau Pinang, Malaysia*

<sup>†</sup>*Institute of Nano-optoelectronics Research  
University of Science Malaysia  
11800 USM, Pulau Pinang, Malaysia*

<sup>‡</sup>*School of Distance Education  
University of Science Malaysia  
11800 USM, Pulau Pinang, Malaysia*

<sup>§</sup>*Science Faculty, University Putra Malaysia  
43400 Serdang, Selangor, Malaysia*

<sup>¶</sup>iskandarshah@usm.my

<sup>||</sup>nurainnabilah\_razali@yahoo.com

<sup>\*\*</sup>nzaherah@usm.my

<sup>††</sup>norzakiah@usm.my

<sup>‡‡</sup>zulhafizzaini90@gmail.com

<sup>§§</sup>nurlinarusli@gmail.com

<sup>¶</sup>mbnizamani@hotmail.com

<sup>||||</sup>hmk6360@gmail.com

Received 9 July 2017; Revised 10 September 2017; Accepted 26 September 2017; Published 23 October 2017

Quaternary glasses were successfully fabricated using melt quenching technique based on the chemical compound composition  $(x)Bi_2O_3-(0.5-x)ZnO-(0.2)B_2O_3-(0.3)SiO_2$ , where  $(x = 0.1, 0.2, 0.3, 0.4, 0.45)$  mole. The sources of  $SiO_2$  was produced from rice husk ash (RHA) at 99.36% of  $SiO_2$ . The Urbach energy was increased from 0.16 eV to the 0.29 eV as the mole of  $Bi_2O_3$  increased in the glass structure. The indirect energy band gap is indicated in decrement pattern with 3.15 eV towards 2.51 eV. The results of Urbach energy and band gap energy that were obtained are due to the increment of  $Bi^{3+}$  ion in the glass network. The refractive indexes for the prepared glasses were evaluated at 2.36 to 2.54 based on the Lorentz-Lorentz formulation which correlated to the energy band gap. The calculated of molar polarizability, electronic polarizability and optical basicity exemplify fine complement to the  $Bi_2O_3$  addition in the glass network. The glass sample was indicated in amorphous state.

**Keywords:** Urbach energy; energy band gap; optical polarizability; Lorentz-Lorentz; X-ray powder diffraction.

### 1. Introduction

Rice Husk Ash (RHA) is an agricultural by-product material that consists about 20% of the weight of rice, 50% cellulose, 25–30% lignin and 15–20% of silica. RHA was generated from the burning of Rice Husk (RH). Therefore, the cellulose and lignin were removed leaving behind silica ash. The better quality of RHA was dependent on the controlled temperature and its particle size and specific surface area were dependent on the burning condition. The color of the complete burn of RH was grey to white ash. Although, the partially-burnt RH was in black (ash).<sup>1</sup>

Usually, silica was obtained as a component of cells or cell wall in virtually all the arial parts of the rice plant but it was abundant in RH. The powdered silicon was obtained from the magnesium reduction of RHA at temperature of 600°C–650°C.<sup>2</sup> Then, the sintered RHA can be a replacement of the silica source in the fabrication of a silicate based glass. The density and refractive index of glass obtained from RHA was higher compared to the  $SiO_2$  glass. The molecular weight of RHA was not considerably different from the pure  $SiO_2$ . Nevertheless, a variety of ions in RHA can be filled in the holes in the glass system and it effects to increase in density.

Based on the classical dielectric theory, the refractive index depends on the density and on the polarizability of the atom in the materials.<sup>3</sup>

The heavy oxide (HMO) glasses like  $\text{Bi}_2\text{O}_3$  and  $\text{PbO}$  have an interesting study in the opto-physical and technology applications. The two oxides can be used for a good glass formation with the combination with different glass formers and modifiers.<sup>4</sup>  $\text{Bi}_2\text{O}_3$  glasses have a high polarizability, low softening point, high refractive index and high density.<sup>5</sup> An electronic polarizability of ions showed the deformation of their electronic clouds due to application of the electromagnetic fields. It was associated to many properties of the materials like refraction, conductivity, ferroelectricity, electro-optical effect, optical basicity along with optical nonlinearity.<sup>6</sup> In this paper, the researcher was focused on the optical properties of quaternary glass based on  $(x)\text{Bi}_2\text{O}_3-(0.5-x)\text{ZnO}-(0.2)\text{B}_2\text{O}_3-(0.3)\text{SiO}_2$ , where  $(x = 0.1, 0.2, 0.3, 0.4 \text{ and } 0.45)$ .

## 2. Experiment Procedure

### 2.1. Preparation of $\text{SiO}_2$

The  $\text{SiO}_2$  used throughout the fabrication process is achieved from RH. Several methods and techniques have been proposed in gaining the maximum percentage of  $\text{SiO}_2$  with adequate amount for fabrication.<sup>7</sup> In this research work, the  $\text{SiO}_2$  preparation method has been improved in order to gain the highest percentage of  $\text{SiO}_2$ . RHs were weighted at 50 g using electronic balance with an accuracy of 0.0001 g, and was rinsed with distilled water to remove dirt by using conical flask and filter paper. After that, the cleaned RH were mixed with 0.4 M of hydrochloric acid HCl in the ratio of 50 g of RH towards 500 ml of HCl, stirred for 20 min with heating temperature of 60°C for 3 h. Then, the RH was rinsed with distilled water to dilute and fully remove the HCl acid. The RH was dried at 100°C for 3 h by using oven. Once dried, the RH was placed in alumina crucibles and burned at 550°C for 6 h, 600°C for 5 h, 700°C for 5 h and 800°C for 4 h to get the white powder of RHA. The RHA were tested using S8 Tiger X-Ray Fluorescence (XRF) Bruker instrument for elemental analysis. The structural phase of RHA was tested by using XRD.

### 2.2. Glass fabrication

The quaternary glass of  $(x)\text{Bi}_2\text{O}_3-(0.5-x)\text{ZnO}-(0.2)\text{B}_2\text{O}_3-(0.3)\text{SiO}_2$ , where  $(x = 0.1, 0.2, 0.3, 0.4 \text{ and } 0.45)$  was fabricated using the conventional melt-quenching method. The oxides' powder mixture was then thoroughly mixed in an agate mortar and pestle for half an hour. The oxides powder mixture was poured into an alumina crucible. The crucible was transferred to a furnace and heated at 1100°C for 1 h 30 min to aid the melting process. When the melting process was completed, the molten liquid was cast into a stainless

steel cylindrical shape mould and annealed at 250°C for 1 h 30 min. A lapping machine is used for grinding and polishing purposes. The glass samples were ground using the Buehler's silica carbide paper at 800 grit towards a preferable parallel thickness of approximately 3.5 mm for required measurements. Two opposite surfaces of each sample were finished optically flat parallel using the 1200 grit silicon carbide paper.

### 2.3. Glass characterization method

The density of glass sample was measured by using the density determination kit. The density of a solid was obtained by averaging the measured values. The density was calculated by using the Archimedes' Principle in Eq. (1).

$$\rho = \frac{A}{|B|} \times \rho_0, \quad (1)$$

where  $A$  is weight of sample in air (g),  $B$  is [weight of sample in air (g)–weight of sample in liquid (g)] and  $\rho_0$  is density of distilled water ( $\text{g/cm}^3$ ). The density of distilled water is 0.99678  $\text{g/cm}^3$ .

The optical properties of the glass sample were measured by using the UV-Visible NIR Spectrophotometer, Model AU12370013 Cary 5000. The UV-Visible NIR spectrophotometer is setup at absorption mode. The range of the wavelength that was used was from 200 nm to 1500 nm and these measurements are made on polished parallel surface bulk glass.

## 3. Result and Discussion

### 3.1. Rice husk compositions

RH is with soaked with 0.4 M of HCl to reduce the contamination inside the RH.<sup>8</sup> After that, the RH was treated at different temperatures that were 550°C, 600°C, 700°C and 800°C to establish the suitable temperature that can obtain an elevated amount of  $\text{SiO}_2$  by reduction of the carbonaceous materials present inside the samples.<sup>9</sup> The RHA samples were analyzed by using XRF measurement to achieve the element and oxide percentage composition within the samples. The data achieved for the highest amount of silica dioxide was demonstrated in at 550°C for 6 h. The highest amount of silica obtained is 99.36%, while other percentages are indicated for the impurity elements in the RHA as illustrated in Table 1.

The amount of  $\text{SiO}_2$  is decreased as the calcination temperature increases as shown in Table 2. It is assumed that the percentages of  $\text{SiO}_2$  decreased due to the solid state reactions between the active RH silica with the impurities within the ash.<sup>10</sup>

Figure 1 illustrates XRD diffractogram pattern of the amorphous RHA obtained from 0.4 M HCl treatment at 550°C within 6 h. The amorphous  $\text{SiO}_2$  was due to the

Table 1. Elemental percentages in RHA with 0.4 M of HCl treatment and 550°C calcination temperature within 6 h.

| Element         | SiO <sub>2</sub> | P <sub>2</sub> O <sub>5</sub> | SO <sub>3</sub> | Na <sub>2</sub> O | CaO  | K <sub>2</sub> O | MgO  | Al <sub>2</sub> O <sub>3</sub> | Cl   | Fe <sub>2</sub> O <sub>3</sub> |
|-----------------|------------------|-------------------------------|-----------------|-------------------|------|------------------|------|--------------------------------|------|--------------------------------|
| Percentages (%) | 99.36            | 0.16                          | 0.10            | 0.06              | 0.15 | 0.05             | 0.04 | 0.03                           | 0.01 | 0.03                           |

Table 2. Percentages of SiO<sub>2</sub> at various calcination temperatures and time.

| Temperature, °C | Time, hours | Percentages of SiO <sub>2</sub> , % |
|-----------------|-------------|-------------------------------------|
| 550             | 6           | 99.36                               |
| 600             | 5           | 99.23                               |
| 700             | 5           | 98.89                               |
| 800             | 4           | 98.82                               |

carbonization temperature to avoid any transformation of amorphous to crystalline form.<sup>9</sup> The main phase displayed the cristobalite. The RHA may have an amorphous form at the combustion temperatures of up to 900°C with 1 h of combustion period. A related point to consider is that the RHA will be of crystalline structure if the temperature exceeds more than 1000°C, for more than 5 min of combustion.<sup>11</sup>

### 3.2. Glass fabrication

The thickness range of the glass (x)Bi<sub>2</sub>O<sub>3</sub>–(0.5 – x) ZnO–(0.2) B<sub>2</sub>O<sub>3</sub>–(0.3)SiO<sub>2</sub> quaternary glass system prepared was around 3.405 mm. The B<sub>2</sub>O<sub>3</sub> and SiO<sub>2</sub> were glass formers in the glass sample. Whereas, the ZnO is like a glass modifier and Bi<sub>2</sub>O<sub>3</sub> is a glass intermediate in the glass sample. The glass sample prepared follows the Zachariasen's Rules. Based on Zachariasen's Rules, no oxygen atom may be linked to more than two cations, the cation coordination number is small, oxygen polyhedral share corners not edged or faces

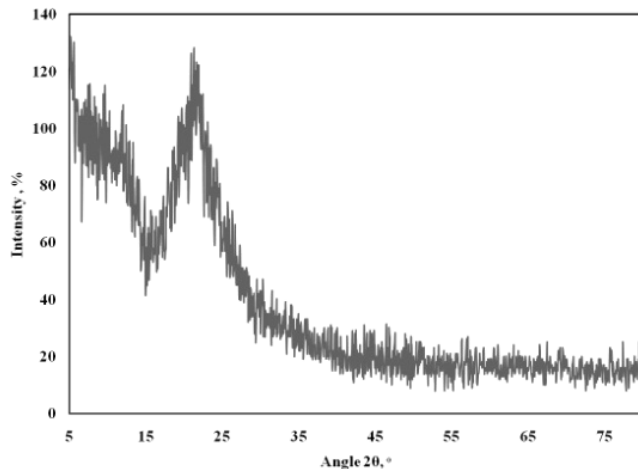


Fig. 1. The XRD diffractogram pattern of RHA for 550°C at 6 h, (JCPDS reference code: 01-076-0938).

and for 3D networks at least their corners must be shared.<sup>12</sup> The color of the glass obtained is from light brown to light yellow, which is dependent on the mole percentages of Bi<sub>2</sub>O<sub>3</sub> and ZnO. The color of glass changes due to the concentration of ZnO in the glass system that can diminish the brown color of the glass sample. Thus, when the mole percentages of Bi<sub>2</sub>O<sub>3</sub> decreased alternately with ZnO increment, the glass coloring also alters from dark brown to light yellow. The color changes of glass were also found in the ternary glass by the previous researcher.<sup>13</sup>

### 3.3. Optical band gap and Urbach energy

The absorption coefficient near the band edge for noncrystalline materials describe the exponential dependence on the photon energy ( $\hbar\omega$ ) which follows the Urbach formula as in Eq. (2).<sup>14</sup>

$$\alpha(\omega) = \alpha_0 \exp(\hbar\omega/E_u), \quad (2)$$

where  $E_u$  is called Urbach energy.

The direct band gap and indirect band gap is the formula given below as

$$\alpha(\omega) = B(\hbar\omega - E_g)^n/\hbar\omega, \quad (3)$$

where  $\hbar\omega$  is the energy of the incident photons,  $E_g$  is the value of the optical gap between valence band and the conduction band and  $n$  is the power which described the electronic transition. It is also whether direct or indirect band gap during the absorption process in the  $K$ -space, where  $n$  is 1/2, 3/2, 2 and 3 was for direct allowed, direct forbidden, indirect allowed and indirect forbidden transitions. The factor  $B$  depends on the transition probability and can be believed to be a constant within the optical frequency range. The graph of  $(\alpha\hbar\omega)^{1/n}$  against  $\hbar\omega$  for  $n = 2$ , is an indirect transition in the amorphous material and  $n = 1/2$  is a direct transition.<sup>14</sup> The absorbance of (x)Bi<sub>2</sub>O<sub>3</sub>–(0.5 – x) ZnO–(0.2)B<sub>2</sub>O<sub>3</sub>–(0.3)SiO<sub>2</sub> glass sample is shown in Fig. 2. The wavelength of absorbance was at the range of 200 nm to 1100 nm. The absorbance peak was increased with increased Bi<sub>2</sub>O<sub>3</sub> in the glass sample.

As illustrated in Fig. 3, the indirect band gap decreases from 3.15 eV to 2.51 eV with an increment of Bi<sub>2</sub>O<sub>3</sub> % mol in the glass network. It is also resulting in the augmentation of Urbach energy in Fig. 3, ranging from 0.16 eV to 0.29 eV. The shift of the UV absorption edge corresponds to transition to the Bi–O bonds which bind an excited electron less compactly than a nonbridging oxygen, and lead to an increase in the value of the energy band gap.<sup>15</sup> The Bi–O bonds are

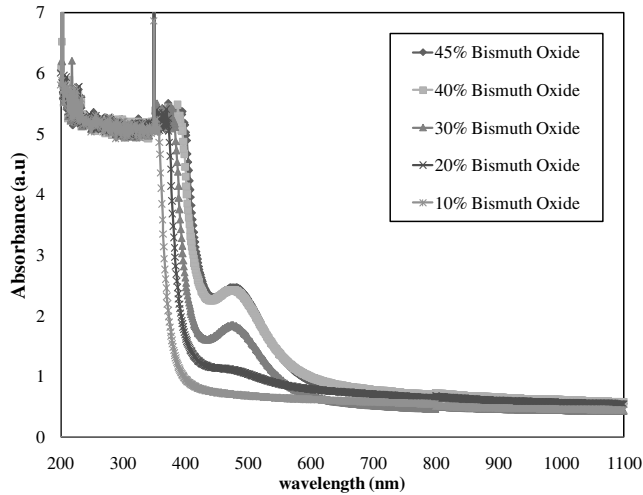


Fig. 2. Absorbance of  $(x)\text{Bi}_2\text{O}_3-(0.5-x)\text{ZnO}-(0.2)\text{B}_2\text{O}_3-(0.3)\text{SiO}_2$  glass sample.

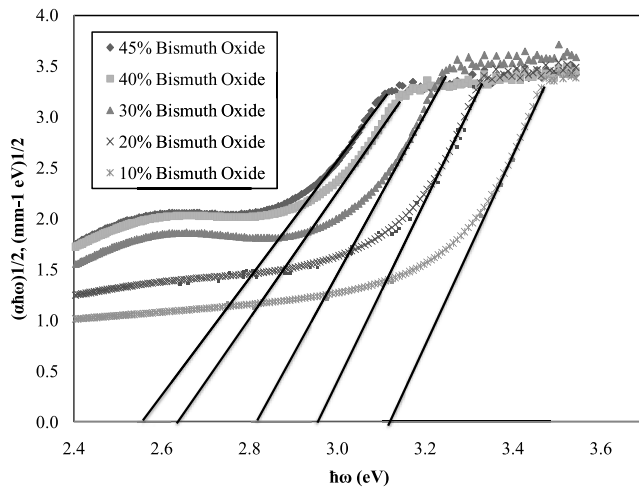


Fig. 3. Indirect band gap of  $(x)\text{Bi}_2\text{O}_3-(0.5-x)\text{ZnO}-(0.2)\text{B}_2\text{O}_3-(0.3)\text{SiO}_2$  glass sample.

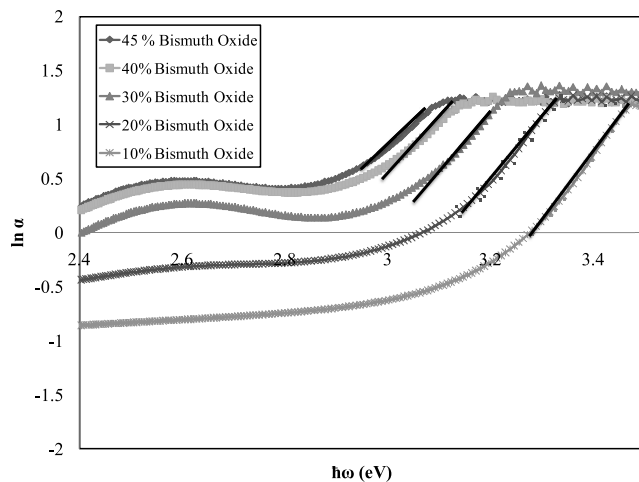


Fig. 4. Urbach energy of  $(x)\text{Bi}_2\text{O}_3-(0.5-x)\text{ZnO}-(0.2)\text{B}_2\text{O}_3-(0.3)\text{SiO}_2$  glass samples.

weaker than pure ionic bonds because they are a covalent bond. Consequently, the oxygen ions can jump into any vacancies liberally. The Urbach energy was used to characterize the degree of disorder in amorphous and crystalline solids. Higher Urbach energy,  $E_u$  attributed towards high number of defects in glass systems.<sup>16</sup> The materials which have large value of  $E_u$  would have greater tendency to convert weak bonds into defects. The width of the band tails ( $E_u$ ) associated with the valance and conduction bands originated from the electron transition between the localized states, where the density of these localized states is exponentially dependent on energy. It was suggested that the Urbach energy arises from the random potential fluctuations in the material into the band gap and normally shows exponential behavior. It has been reported that the experimental tail observed in various materials with different structures have the same physical origin and this can be attributed to the phonon-assisted indirect electronic transition.<sup>15</sup>

### 3.4. Refractive index, molar polarizability, electrical polarizability and optical basicity

Refractive index was determined from an optical energy band gap by using Eq. (4).

$$\frac{n^2 - 1}{n^2 + 2} = 1 - \sqrt{\frac{E_{\text{opt}}}{20}} \quad (4)$$

The electronic polarizability glasses can be calculated by using the Lorentz–Lorentz equation that used the relationship between molar refraction,  $R_m$ , refractive index and density.

$$R_m = \left[ \frac{n^2 - 1}{n^2 + 2} \right] \left( \frac{M}{\rho} \right) = \left[ \frac{n^2 - 1}{n^2 + 2} \right] V_m = \frac{4\pi\alpha_m N}{3} \quad (5)$$

where  $M$  is the molecular weight,  $V_m$  is the molar volume,  $\alpha_m$  is the molar polarizability and  $N$  is the Avogadro’s number. The molar polarizability is based on the magnitude of electrons that responds to an electrical field represented by the Lorentz–Lorentz equation. Within  $\alpha_m$  in ( $\text{\AA}^3$ ) in Eq. (5) can be functionally altered to the following expression:

$$\alpha_m = \frac{R_m}{2.52} \quad (6)$$

The Lorentz–Lorentz equation allows the computation of the electronic polarizability of the oxide ions,  $\alpha_{o2-}(n)$ , in the oxide materials by subtracting the cation polarizability from molar polarizability  $\alpha_m$  as indicated in the following equation:

$$\alpha_{o2-}(n) = \left[ \frac{R_m}{2.52} - \sum \alpha_i \right] (N_{o2-})^{-1} \quad (7)$$

where  $\sum \alpha_i$  denotes molar polarizability, and denotes the number of oxide ions in the chemical formula. The value for  $\alpha_{\text{Bi}} = 1.508$  for  $\text{Bi}^{3+}$ ,  $\alpha_{\text{Zn}} = 0.283$  for  $\text{Zn}^+$ ,  $\alpha_{\text{B}} = 0.002$  for  $\text{B}^{3+}$ ,  $\alpha_{\text{Si}} = 0.033$  for  $\text{Si}^{2+}$ .

Table 3. The value of density, molar volume, oxygen packing density, refractive index, indirect band gap, direct band gap, Urbach energy, molar polarizability, electronic polarizability, optical basicity and molar refraction of  $(x)\text{Bi}_2\text{O}_3-(0.5-x)\text{ZnO}-(0.2)\text{B}_2\text{O}_3-(0.3)\text{SiO}_2$  glass samples.

| Physical and optical properties        | Bi <sub>2</sub> O <sub>3</sub> Mole percentage |              |              |              |              |
|--|--|--------------|--------------|--------------|--------------|
|  | 10%  | 20%          | 30%          | 40%          | 45%          |
| Density, g/cm <sup>3</sup>             | 4.59 ± 0.009                                   | 4.97 ± 0.011 | 5.87 ± 0.006 | 6.20 ± 0.033 | 6.31 ± 0.014 |
| Molar volume, cm <sup>3</sup>          | 24.21  | 30.10        | 32.03        | 36.53        | 38.94        |
| Oxygen packing density                 | 78.48  | 69.78        | 71.80        | 68.43        | 66.78        |
| Refractive index                       | 2.36   | 2.41         | 2.45         | 2.52         | 2.54         |
| Indirect band gap, eV                  | 3.15   | 2.95         | 2.80         | 2.59         | 2.51         |
| Urbach energy, eV                      | 0.16   | 0.19         | 0.21         | 0.25         | 0.29         |
| Molar polarizability                   | 5.93   | 7.23         | 8.68         | 9.41         | 9.49         |
| Electronic polarizability of oxide ion | 3.19   | 3.88         | 4.59         | 4.76         | 4.67         |
| Optical basicity                       | 1.15   | 1.24         | 1.30         | 1.32         | 1.31         |
| Molar refraction                       | 15.06  | 18.29        | 21.95        | 23.78        | 24.00        |

The optical basicity had the following relationship between the electronic polarizability:

$$\Lambda = 1.67 \left( 1 - \frac{1}{\alpha_{o2-}} \right). \quad (8)$$

The values of density, molar volume, oxygen packing density, refractive index, indirect band gap, direct band gap, Urbach energy, molar polarizability, electronic polarizability, optical basicity and molar refraction of  $(x)\text{Bi}_2\text{O}_3-(0.5-x)\text{ZnO}-(0.2)\text{B}_2\text{O}_3-(0.3)\text{SiO}_2$  glass samples are summarized in Table 3.

Density and molar volume was increased as the percentage mole of Bi<sub>2</sub>O<sub>3</sub> increased, as the molecular weight of Bi<sub>2</sub>O<sub>3</sub> is higher than ZnO, B<sub>2</sub>O<sub>3</sub> and SiO<sub>2</sub>, and atomic number of Bi<sup>3+</sup> is higher than Zn<sup>2+</sup>, B<sup>3+</sup> and Si<sup>2+</sup>, and the augmentation in bond length increased the bond length or the inter atomic spacing between atoms.<sup>16</sup> While the oxygen packing density decreased due to the nonbridging oxygen atom, which increased due to the higher atomic number of Bi<sup>3+</sup> in the glass system.<sup>17</sup> The refractive index was used to find the suitability of the glass materials to be used for optical devices. Refractive index was calculated by using the relationship between the band gap energy. There are a few factors that affected the refractive index: (1) polarizability of the neighboring ions coordinated with it (anion); (2) coordination number of the ion; (3) electronic polarizability of the glass oxide ion; (4) optical basicity of the glasses.<sup>18</sup> The refractive index increased with increase in Bi<sub>2</sub>O<sub>3</sub> content in glass samples as illustrated in Table 3. The increases in refractive index is due to the decreases in oxygen packing density which create more nonbridging oxygen in the glass samples. Therefore, the enlarged value of the nonbridging oxygen possesses a greater number of polarizability which results in the escalating in refractive index.

Based on Fig. 5, the molar polarizability of glass samples increased towards the plateau as Bi<sub>2</sub>O<sub>3</sub> content increased. It was increasing proportionally with the increment of molar refraction and refractive index of the glass samples. Molar

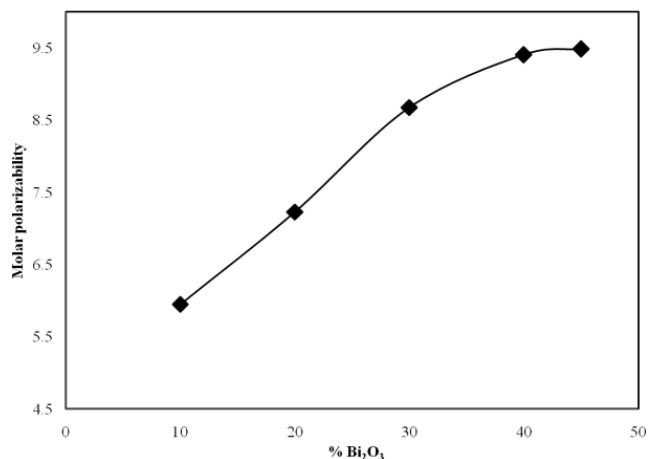


Fig. 5. The molar polarizability of  $(x)\text{Bi}_2\text{O}_3-(0.5-x)\text{ZnO}-(0.2)\text{B}_2\text{O}_3-(0.3)\text{SiO}_2$  glass sample.

polarizability was calculated by using Eq. (4). The electronic polarizability of oxide ions was increased as the molar polarizability increased as shown in Fig. 6.

The optical basicity of glass samples was increased towards the plateau as the electronic polarizability of oxide ions increases as shown in Fig. 7. The optical basicity of an oxide medium is the numerical expression of the average electron donor power of the oxide species constituting the medium. The increasing in the electronic polarizability of oxide ions indicates the stronger ability of the electron donor of the oxide ions. The optical basicity give an information about the acid-based properties of oxides, glasses, alloys, molten salts and others.<sup>19</sup> According to Leboutellier and Courline (ALC),<sup>6</sup> the values of optical basicity of each oxide are:  $\Lambda(\text{B}_2\text{O}_3) = 0.42$ ,  $\Lambda(\text{Bi}_2\text{O}_3) = 1.19$ ,  $\Lambda(\text{ZnO}) = 0.92$ ,  $\Lambda(\text{Si}_2\text{O}_3) = 0.48$ . The values indicate that Bi<sub>2</sub>O<sub>3</sub> has larger values than other elements in glass samples. The increased optical basicity is due to the higher number of Biatom (1.19) in the glass samples. Therefore, the value of refractive index, molar

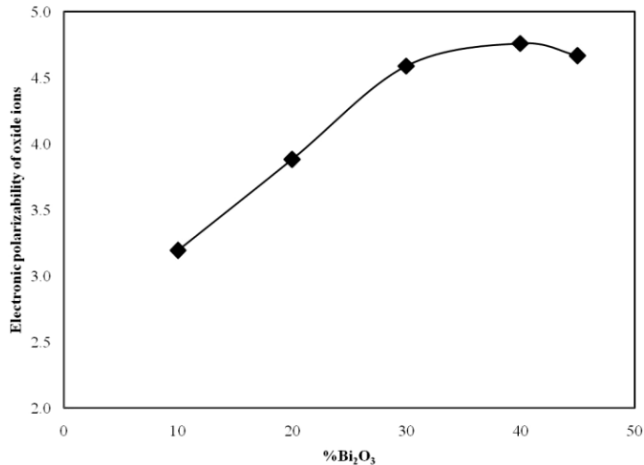


Fig. 6. The electronic polarizability of oxide ions in  $(x)\text{Bi}_2\text{O}_3-(0.5-x)\text{ZnO}-(0.2)\text{B}_2\text{O}_3-(0.3)\text{SiO}_2$  glass sample

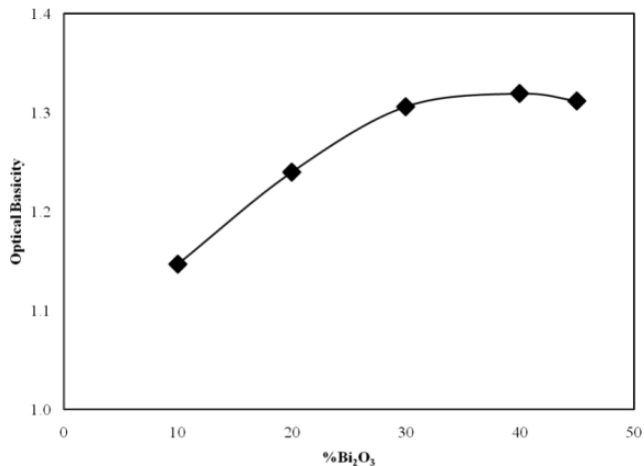


Fig. 7. The optical basicity of  $(x)\text{Bi}_2\text{O}_3-(0.5-x)\text{ZnO}-(0.2)\text{B}_2\text{O}_3-(0.3)\text{SiO}_2$  glass sample.

polarizability, electronic polarizability of oxide ions and optical basicity in the  $(x)\text{Bi}_2\text{O}_3-(0.5-x)\text{ZnO}-(0.2)\text{B}_2\text{O}_3-(0.3)\text{SiO}_2$  glass samples display sole dependency towards the  $\text{Bi}_2\text{O}_3$  concentration.

### 3.5. XRD of glass sample

The crystalline or amorphous nature of solids can be different by the degree of geometric order of the constituent molecules. Amorphous solids show a lack of structural arrangement and are known as super-cooled liquids since their atomic structure is like a liquid. While a solid is heated, it's ordered molecular lattice elements vibrate with increasing frequency until the melting point of the material is approached.<sup>20</sup> The XRD result showed that the glass samples have an amorphous nature as shown in Fig. 8 with the presence of hump from 20° to 35°.

The hump becomes sharper as the content of  $\text{Bi}_2\text{O}_3$  varies due to the number of density of crystals with high  $\text{Bi}_2\text{O}_3$

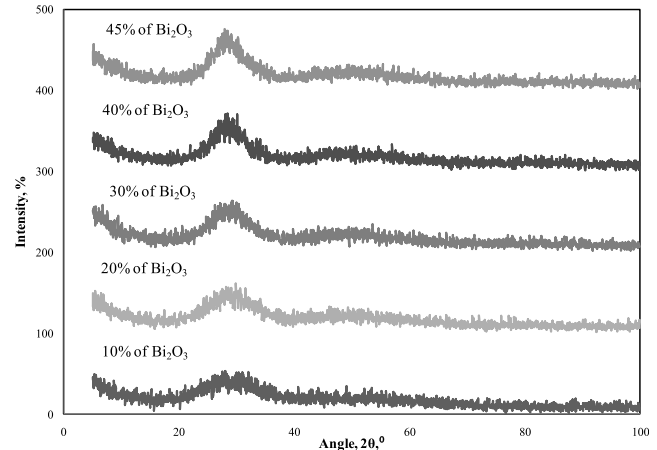


Fig. 8. The XRD spectrum of  $(x)\text{Bi}_2\text{O}_3-(0.5-x)\text{ZnO}-(0.2)\text{B}_2\text{O}_3-(0.3)\text{SiO}_2$  glass sample.

content. Therefore, the increment in a crystal fraction with Bi content, is the Bi ions directly attaching to the formation of crystal nuclei in the glass as it is being quenched from the melt. The crystal nuclei developed during treatment were first produced in the Bi ions' rich phases in glass.<sup>21</sup>

## 4. Conclusions

High purity (99.36%) of  $\text{SiO}_2$  from RH treatment was successfully obtained and used for the glass fabrication process of  $(x)\text{Bi}_2\text{O}_3-(0.5-x)\text{ZnO}-(0.2)\text{B}_2\text{O}_3-(0.3)\text{SiO}_2$ . The optical properties via energy band gap, Urbach energy, refractive index, molar polarizability, electronic polarizability of oxide ions and optical basicity of the glass system have been studied. It is found that the optimal parameterization achieved dependent on the glass composition, especially on the percentage of  $\text{Bi}_2\text{O}_3$ .

## Acknowledgment

The author acknowledges the University Science Malaysia for the financial support for this research under two USM (Short Term Grant) which are 304/PFIZIK/6313152 and 304/PFIZIK/6313249.

## References

- <sup>1</sup>R. Siddique, Cement Kiln dust, in *Waste Materials and By-Products in Concrete* (Springer, Berlin, 2008), pp. 351–380.
- <sup>2</sup>R. Patil, R. Dongre and J. Meshram, Preparation of silica powder from rice husk, *J. Appl. Chem.* **27**, 26 (2014).
- <sup>3</sup>Y. Ruangtaweep, J. Kaewkhao, K. Kirdsiri, C. Kedkaew and P. Limsuwan, Properties of CoO doped in glasses prepared from rice hush fly ash in Thailand, *IOP Conf. Ser. Mater. Sci. Eng.* **18**(11), 112008 (2011).
- <sup>4</sup>M. A. Chaudhry, Thermal stability and band gap study of heavy metal oxy-sulfide glass system, *J. Therm. Anal. Calorim.* **112**(2), 539 (2013).

- <sup>5</sup>S. P. Singh and B. Karmakar, Synthesis and characterization of low softening point high Bi<sub>2</sub>O<sub>3</sub> glasses in the K<sub>2</sub>O–B<sub>2</sub>O<sub>3</sub>–Bi<sub>2</sub>O<sub>3</sub> system, *Mater. Character.* **62**(6), 626 (2011).
- <sup>6</sup>V. Dimitrov and T. Komatsu, An interpretation of optical properties of oxides and oxide glasses in terms of the electronic ion polarizability and average single bond strength, *J. Univ. Chem. Technol. Metall.* **45**(3), 219 (2010).
- <sup>7</sup>I. S. Mustafa, N. A. N. Razali, A. R. Ibrahi, N. Z. Yahay and H. M. Kamari, From rice husk to transparent radiation protection material, *J. Intelek* **9**(2), 1 (2015).
- <sup>8</sup>J. P. Nayak and J. Bera, Effect of sintering temperature on phase formation behavior and mechanical properties of silica ceramics prepared from rice husk ash, *Phase Transit.* **82**(12), 879 (2009).
- <sup>9</sup>V. P. Della, I. Kühn and D. Hotza, Rice husk ash as an alternate source for active silica production, *Mater. Lett.* **57**(2), 818 (2002).
- <sup>10</sup>L. Xiong, E. H. Sekiya, P. Sujaridworakun, S. Wada and K. Saito, Burning temperature dependence of rice husk ashes in structure and property, *J. Met. Mater. Miner.* **19**(2), 95 (2017).
- <sup>11</sup>D. G. Nair, A. Fraaij, A. A. Klaassen and A. P. Kentgens, A structural investigation relating to the pozzolanic activity of rice husk ashes, *Cement Concrete Res.* **38**(6), 861 (2008).
- <sup>12</sup>M. Lopes and J. E. Shelby, *Introduction to Glass Science and Technology* (Royal Society of Chemistry, Cambridge, 2005).
- <sup>13</sup>J. Hooda, R. Punia, R. S. Kundu, S. Dhankhar and N. Kishore, Structural and physical properties of ZnO modified bismuth silicate glasses, *ISRN Spectrosc.* **2012**, Article ID 578405 (5 pages) (2012), doi:10.5402/2012/578405.
- <sup>14</sup>M. F. Zaki, Gamma-induced modification on optical band gap of CR-39 SSNTD, *J. Phys. D Appl. Phys.* **41**(17), 175404 (2008).
- <sup>15</sup>V. Kundu, R. L. Dhiman, A. S. Maan and D. R. Goyal, Optical and spectroscopic studies of ZnO–Bi<sub>2</sub>O<sub>3</sub>–B<sub>2</sub>O<sub>3</sub> glasses, *J. Optoelectron. Adv. Mater.* **11**(11), 1595 (2009).
- <sup>16</sup>M. K. Halimah, W. M. Daud, H. A. A. Sidek, A. W. Zaidan and A. S. Zainal, Optical properties of ternary tellurite glasses, *Mater. Sci. Pol.* **28**(1), 173 (2010).
- <sup>17</sup>S. Rakpanich, P. Meejitpaisan and J. Kaewkhao, Physical, Optical and Luminescence Properties of Er<sup>3+</sup>-Doped Bismuth Borosilicate Glasses, *Key Eng. Mater.* **675**, 372 (2016).
- <sup>18</sup>M. N. Azlan, M. K. Halimah, S. Z. Shafinas and W. M. Daud, Polarizability and optical basicity of Er<sup>3+</sup> ions doped tellurite based glasses, *Chalcogenide Lett.* **11**(7), 319 (2014).
- <sup>19</sup>T. Komatsu, N. Ito, T. Honma and V. Dimitrov, Electronic polarizability and its temperature dependence of Bi<sub>2</sub>O<sub>3</sub>–B<sub>2</sub>O<sub>3</sub> glasses, *J. Non-Cryst. Solids* **356**(44), 2310 (2010).
- <sup>20</sup>R. T. Chancey, *Characterization of Crystalline and Amorphous Phases and Respective Reactivities in a Class F Fly Ash* (University of Texas, Austin, 2008).
- <sup>21</sup>X. Hu, G. Guery, J. Boerstler, J. D. Musgraves, D. Vanderveer, P. Wachtel and K. Richardson, Influence of Bi<sub>2</sub>O<sub>3</sub> content on the crystallization behavior of TeO<sub>2</sub>–Bi<sub>2</sub>O<sub>3</sub>–ZnO glass system, *J. Non-Cryst. Solids* **358**(5), 952 (2012).